2260–2267 *Nucleic Acids Research, 2001, Vol. 29, No. 11*

Triple-helix formation in the antiparallel binding motif of oligodeoxynucleotides containing N^9- and N^7-2-aminopurine deoxynucleosides

Serge P. Parel and Christian J. Leumann*

Department of Chemistry and Biochemistry, University of Berne, Freiestrasse 3, CH-3012 Berne, Switzerland

Received March 5, 2001; Revised and Accepted April 11, 2001

ABSTRACT

Triplex-forming oligodeoxynucleotide 15mers, designed to bind in the antiparallel triple-helical binding motif, containing single substitutions (Z) of the four isomeric αN^7-, βN^7-, αN^9- and βN^9-2-aminopurine (ap)-deoxyribonucleosides were prepared. Their association with double-stranded DNA targets containing all four natural base pairs (X-Y) opposite the aminopurine residues was determined by quantitative DNase I footprint titration in the absence of monovalent metal cations. The corresponding association constants were found to be in a rather narrow range between 1.0×10^6 and 1.3×10^8 M^{-1}. The following relative order in Z × X-Y base-triple stabilities was found: Z = αN^7ap: T-A > A-T> C-G ~ G-C; Z = βN^7ap: A-T > C-G > G-C > T-A; Z = αN^9ap: A-T = G-C > T-A > C-G; and Z = βN^9ap: G-C > A-T > C-G > T-A.

INTRODUCTION

Strong and sequence-specific triple-helix formation of oligonucleotides with genomic DNA can selectively interfere with gene expression at the level of transcription and is therefore of interest in medicinal chemistry and biotechnology (1–2). However, the molecular recognition of a DNA duplex via a triplex forming oligonucleotide (TFO) in either the parallel (3–4) or the antiparallel (5–6) binding motif is limited to homopurine–homopyrimidine DNA sequence tracts. Despite considerable efforts over the past decade to overcome this sequence restriction by TFO design, a general solution to the problem still remains elusive (7).

A number of third-strand design options to overcome this sequence restriction have been investigated in the past. In order to recognize DNA duplexes containing purine–pyrimidine block sequence intervals, TFOs binding via a combination of the purine and the pyrimidine motif (8–9), as well as TFOs with 3′–3′- or base–base junctions were studied (10–15). Furthermore, TFOs containing extended nucleobases spanning a complete Watson–Crick base pair in the major groove (16,17), and base-modified TFOs selectively recognizing pyrimidine bases (18–22), were investigated. In all of these cases, either the affinity of the corresponding TFOs to their target, or the selectivity in base pair recognition, or both did not fulfill the required criteria for broad application in DNA-based therapy and diagnosis.

A particularly intriguing conceptual approach is the design of TFOs with a structural switch, enabling the bases to cross the major groove and target consecutive purine bases on either strand of the target duplex. One such switch model consists of the consecutive use of α- and β-configured nucleotides (α,β-switch model). The α,β-switch model had been proposed earlier (23), and was recently investigated experimentally in the context of alternate strand G recognition by α-, and β-4-guanidinopyrimidine-containing oligonucleotides (24,25), without success, however. In this communication we report on an alternative design and experimental evaluation of such switch TFOs.

MATERIALS AND METHODS

Oligonucleotide synthesis

Oligonucleotide synthesis was performed on a Pharmacia Gene Assembler Special connected to a Compaq ProLinea 3/25-zs PC. All syntheses were performed using the 1.3 μmol cycle with coupling times of 2 min for the 2-aminopurine building blocks. The phosphoramidite building blocks of the four isomeric 2-aminopurine (ap) nucleoside analogs αN^7ap, βN^7ap, αN^9ap and βN^9ap (Fig. 1) were prepared as described by us previously (26). Phosphoramidite solutions (0.1 M in

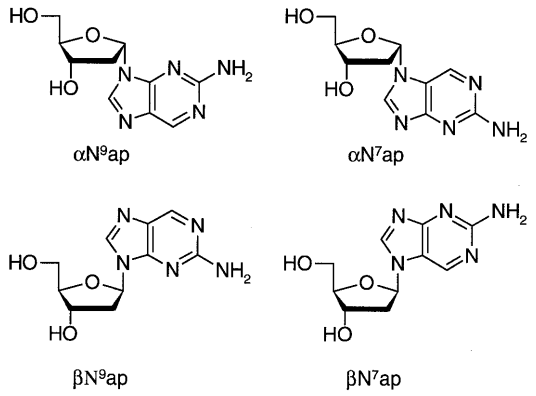

Figure 1. Chemical structures of the isomeric 2-aminopurine nucleosides αN^7ap, βN^7ap, αN^9ap and βN^9ap used in this study.

*To whom correspondence should be addressed. Tel: +41 31 631 4355; Fax: +41 31 631 3422; Email: leumann@ioc.unibe.ch

Table 1. Synthesis and analytical data of oligonucleotides 1–8

Sequence	Isolated yield OD (260 nm) ([%])	Electrospray-MS [M-H]$^-$	
		m/z (calc.)	*m/z* (found)
1 d(GGTGG-αN^{7}ap-GGTTGTGGT)	52 (29)	4734.7	4734.9
2 d(GGTGG-βN^{7}ap-GGTTGTGGT)	80 (45)	4734.7	4734.6
3 d(GGTGG-αN^{9}ap-GGTTGTGGT)	28 (16)	4734.7	4732.1
4 d(GGTGG-βN^{9}ap-GGTTGTGGT)	69 (38)	4734.7	4734.5
5 d(GGTGGTGGTTGTGGT)	71 (40)	4727.9[a]	4727.7[a]

[a]MS measured in ESI$^+$ mode; *m/z* given is for [M+H]$^+$.

MeCN) were equal in concentration to those used for the synthesis of natural oligodeoxynucleotides. The activator 1*H*-tetrazole was replaced in all syntheses by 5-(benzylthio)-1*H*-tetrazole (0.25 M in MeCN) (27). Average coupling yields, monitored by the on-line trityl assay, were >98% for all four 2-aminopurine phosphoramidites. Removal of the protecting groups and detachment from the solid support was effected in concentrated NH_3 solution (1–2 ml) at 55°C for 18–20 h. The crude oligomers were purified by MonoQ ion-exchange HPLC, desalted over Sep-Pak C-18 cartridges (Waters) and their purity and composition confirmed by Electrospray-MS analysis. Table 1 contains synthetic and analytical data of the oligonucleotides described here. All natural DNA sequences used in this study were prepared according to standard phosphoramidite chemistry and purified by HPLC.

T_m measurements

UV-melting experiments were performed on a Varian-Cary-3E UV/Vis spectrometer equipped with a temperature controller unit and connected to a PC running the Varian WinUV software; temperature gradient 0.5°C/min; data-point collection in intervals of ~1°C; below 20°C, the cell compartment was flushed with N_2 to avoid condensation of H_2O on the UV cells; the transition temperature T_m was determined as the maximum of the first derivative of the melting curve using the software package Origin™ v5.0.

Preparation of plasmid pSPP4C1

All DNA and cell manipulations followed standard protocols (28). All aqueous solutions for DNA manipulations were prepared with Milli-Q water (Millipore). *Escherichia coli* XL-1 Blue competent cells were from Stratagene. Sonicated calf thymus DNA, T4 polynucleotide kinase and Sequenase v.2.0 were from AP Biotech. The restriction enzymes were from Roche Diagnostics. T4 DNA ligase was from Sigma. [α-^{32}P]dATP (3000 Ci/mmol, 250 µCi) was from Hartmann Analytik GmbH. Buffers (if not provided with the enzymes) were made from Fluka (Microselect grade) or Sigma chemicals. Synthetic oligonucleotides were prepared as described before at the 0.2 µmol scale using standard β-cyanoethyl phosphoramidites and solid supports (AP Biotech). Modified coupling times of 2 min were used. Oligonucleotides were purified by denaturing polyacrylamide gel electrophoresis.

The DNA duplex containing the four triplex target cassettes was prepared starting with the following set of overlapping

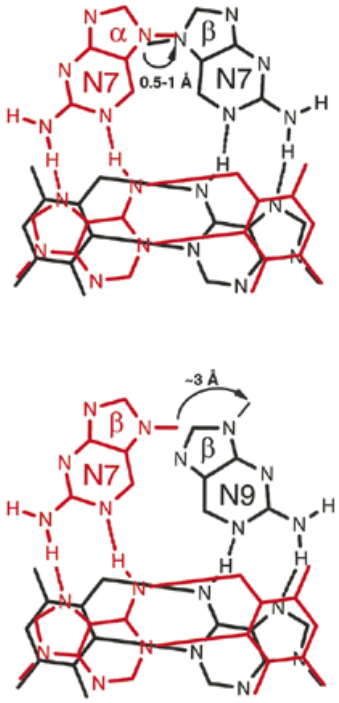

Figure 2. Schematic view of consecutive, alternate strand recognition of adenine bases on a DNA target duplex by aminopurine bases of a TFO, using the α/β-switch model (top) or the N^7/N^9-switch model (bottom). For clarity, only the heteroatoms of the purine bases are drawn.

oligonucleotides: 5′-CGACGACCCGGGACGCTCGACAGGC-**AGGAGAAGGAGGAGG**GTATCAAGACTTCG-3′; 5′-C**AGGAGAAGGCGGAGG**CAACTCACGTTCGGT**AGGAGAAGGTGGAGG**TCTTGAGCTGGCA-3′; 5′-AC**AGGAGAAGGGGGAGG**TACACTGGCCATGACCAAGCTTGCGC-TCTGCTGAAGAAGCCAG-3′; 3′-GCTGCTGGGCCCTGC-GAGCTGTCC-5′; 3′-G**TCCTCTTCCTCCTCC**CATAGT-TCTGAAGCG**TCCTCTTCCGCCTCC**GTTG-5′; 3′-AGT-GCAAGCCA**TCCTCTTCCACCTCC**AGAACTCGACCG TTG**TCCTCTTCCCCCTCC**ATGTG-5′; 3′-ACCGGTAC-TGGTTCGAACGCGAGACGACTTCTTCGGTC-5′.

With the exception of the two 5′-fragments, all oligonucleotides were phosphorylated using ATP and T4 polynucleotide kinase. An equimolar mixture of all oligonucleotides was then equilibrated and ligated using T4 ligase. The resulting duplex was digested with *Hin*dIII and *Ava*I and ligated into the

```
D1      5′-GCTAGGAGAAGGAGGAGGTCG-3′
        3′-CGATCCTCTTCCTCCTCCAGC-5′
1       5′-GGTGG-α-7ap-GGTTGTGGT-3′
2       5′-GGTGG-β-7ap-GGTTGTGGT)-3′
3       5′-GGTGG-α-9ap-GGTTGTGGT)-3′
4       5′-GGTGG-β-9ap-GGTTGTGGT)-3′
5       5′-GGTGGTGGTTGTGGT)-3′
```

Figure 3. Sequences of the duplex target used in the UV-melting curve analyses as well as TFOs 1–5 containing the different isomeric 2-aminopurine nucleosides.

large *Hin*dIII–*Ava*I restriction fragment of pUC18 (→pSPP4C1). Competent *E.coli* XL-1 Blue cells were transformed with the ligated plasmid, and plasmid DNA from ampicillin-resistant white colonies was isolated. The presence of the desired insert of the selected clone was determined by restriction analysis and forward and reversed Sanger dideoxy sequencing. Two mutations (CG→TA at position 55 and CG→GC at position 112 of the original duplex) were detected. The mutations, however, were outside of the target cassettes. The plasmid was isolated on a preparative scale using a Maxi Prep Kit (Qiagen) affording 380 µg of pSPP4C1.

3′-End-labeling of DNA fragments

In a typical end-labeling experiment, 6 µg of plasmid pSPP4C1 were digested with restriction endonucleases *Eco*RI and *Pvu*II and the products were separated by agarose gel electrophoresis. The desired band was excised and extracted with the QiaexII Extraction Kit (Qiagen). The restriction fragment was then ethanol-precipitated and redissolved in H_2O. 3′-End-labeling was performed with [α-^{32}P]dATP using Sequenase (v2.0). Excess unlabeled nucleotide triphosphates (dTTP, dATP) were added after labeling to ensure complete fill in. Non-incorporated nucleotide was removed by gel filtration over NICK columns (AP Biotech). Finally, the labeled fragment was ethanol-precipitated. From ~6 µg of plasmid, a total Cerenkov radioactivity of 4 000 000–15 000 000 c.p.m. was obtained.

DNase I footprint titrations

These experiments were performed according to published protocols (29,30). Typically, TFOs were dissolved in H_2O to a concentration of 25 µM and this solution was serially diluted to a total of 10 concentrations spanning the desired range for the experiment (final concentrations of 300 pM to 10 µM). H_2O was added to adjust the volume to 18 µl. To each tube, 27 µl of a stock solution containing the labeled restriction fragment of

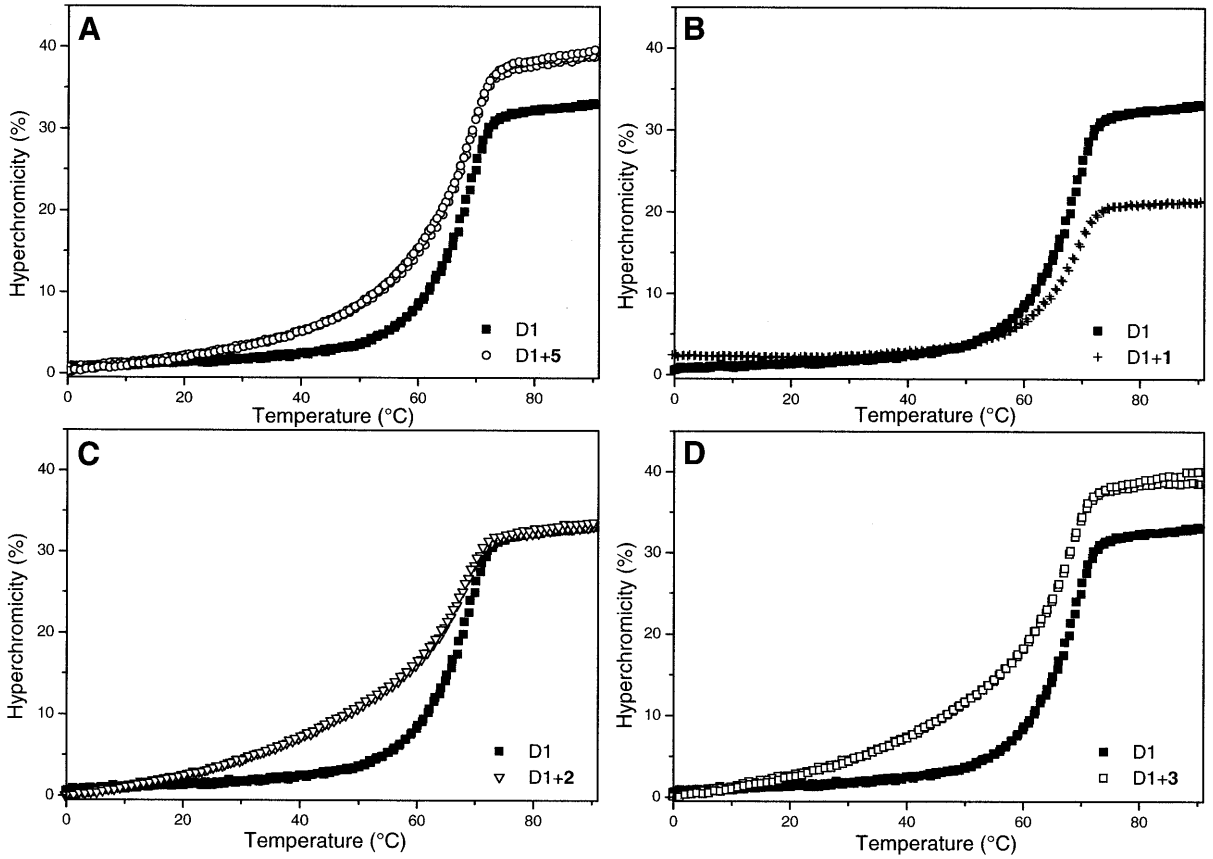

Figure 4. UV-melting curves (280 nm) of duplex D1 with TFOs 1, 2, 3 and 5 in 90 mM Tris–borate pH 7.5, 10 mM $MgCl_2$ (strand concentration = 1.5 µM). Superposition of consecutive heating–cooling–heating cycles in the presence [circles, crosses, inverted triangles and open squares in (**A**), (**B**), (**C**) and (**D**), respectively] and absence (closed squares) of TFO.

Table 2. Association constants K_a (in M^{-1}) reported as the mean (± standard error) of at least three measurements for the triplexes formed by the oligonucleotides 1–5 with the four target cassettes on duplex SPP4C1, where X is on the purine strand and Y is on the pyrimidine strand

		X·Y			
		A·T	C·G	G·C	T·A
	T	1.7 (±0.8)·10^8	1.4 (±0.7)·10^7	2.3 (±1.0)·10^7	5.5 (±4.7)·10^6
Z	βN^{7}ap	5.2 (±0.6)·10^7	2.2 (±1.0)·10^7	7.5 (±6.1)·10^6	5.8 (±5.6)·10^6
	αN^{7}ap	1.1 (±0.5)·10^7	6.9 (±3.1)·10^6	7.3 (±2.5)·10^6	4.2 (±2.6)·10^7
	βN^{9}ap	2.0 (±0.9)·10^7	2.3 (±1.1)·10^6	1.2 (±0.8)·10^8	1.0 (±0.5)·10^6
	αN^{9}ap	1.3 (±0.4)·10^8	2.7 (±1.2)·10^7	1.3 (±0.6)·10^8	5.5 (±2.5)·10^7

For experimental conditions see Figure 5.

Table 3. Standard free energies of triplex formation ($\Delta G°$) at 20°C [kcal·mol^{-1}] derived from the association constants listed in Table 1

		X·Y			
		A·T	C·G	G·C	T·A
	T	–11.1 (±0.2)	–9.6 (±0.3)	–9.9 (±0.1)	–9.1 (±0.4)
Z	βN^{7}ap	–10.4 (±0.1)	–9.9 (±0.2)	–9.3 (±0.3)	–9.1 (±0.4)
	αN^{7}ap	–9.5 (±0.2)	–9.2 (±0.2)	–9.3 (±0.1)	–10.3 (±0.3)
	βN^{9}ap	–9.9 (±0.2)	–8.6 (±0.2)	–10.9 (±0.3)	–8.1 (±0.2)
	αN^{9}ap	–10.9 (±0.2)	–10.0 (±0.2)	–10.9 (±0.3)	–10.4 (±0.3)

pSPP4C1 (20 000 c.p.m.) together with 9 µl 5× association buffer (50 mM bis-Tris–HCl, 50 mM $MgCl_2$, 5 mM spermine tetrahydrochloride, pH 7.2) and H_2O were added (final solution conditions: 10 mM bis-Tris–HCl, 10 mM $MgCl_2$, 1 mM spermine). After 7 days equilibration at 20°C, 2.5 µg sonicated calf thymus DNA was added. The digestion was started by the addition, at room temperature of 5 µl of a solution containing 24 U DNase I (from a 10 U/µl stock solution) in 120 µl digestion buffer [50 mM $CaCl_2$, 50 mM $MgCl_2$, 10 mM bis-Tris–HCl pH 7, 5% glycerine, 10 µM non-specific sequence $^{5'}$d(TATAATTTAA)$^{3'}$]. After 1.5 min, the digestion was quenched by the addition of 8.3 µl of a solution containing 1.4 M NaCl, 0.14 M EDTA pH 8, 0.35 µg/ml glycogene. 20 µl 3 M NaOAc pH 5.2, and 150 µl cold ethanol were added. After 3 h at –20°C, the tubes were centrifuged (30 min, 16 000 *g*, 4°C). The pellets were washed with 80 µl cold 70% ethanol, centrifuged (15 min), solved in 20 µl H_2O, lyophilized and dissolved in 7 µl of 80% formamide loading buffer. After denaturation (10 min, 85°C), the samples were loaded on an 8% denaturing polyacrylamide gel and separated by electrophoresis in 1× TBE buffer at 1900 V for 90 min. After drying on a slab drier (80°C, 1 h) the gel was exposed to a storage PhosphorImager screen (Molecular Dynamics) overnight at ambient temperature.

Quantification and data analysis

Quantification of the footprint titrations was performed as described (30), using ImageQuant v3.3 software (Molecular Dynamics). For the determination of the association constants of the studied triple helices, the following equilibrium and the corresponding equilibrium constant K_a were considered:

$$D + SS \leftrightarrow T$$

$$K_a = [T]/([SS][D])$$

where *D*, *SS* and *T* represent the duplex, single-strand and triplex, respectively.

The apparent fractional occupancy θ_{app} can be calculated as:

$$\theta_{app} = 1 - [(D_{n,XY}/D_{n,out})/(D_{R,XY}/D_{R,out})]$$

with $D_{n,XY}$ being the optical density of target XY (XY = AT, CG, GC or TA) in lane n, $D_{n,out}$ being the optical density of a reference region of lane n (the optical density of the reference region should be more or less constant for all lanes of the gel). $D_{R,XY}$ is the optical density of target XY in the reference lane (no third strand) and $D_{R,out}$ is the optical density of the reference region in the reference lane. The obtained θ_{app} can then be fitted to a sigmoidal curve using the following formula:

$$I_{fit} = \theta_{min,XY} + (\theta_{max,XY} - \theta_{min,XY})\ K_a\ [c/(1 + K_a \times c)]$$

$\theta_{min,XY}$, $\theta_{max,XY}$ and K_a being three variable parameters and *c* the total third strand concentration. The association constant is K_a.

RESULTS AND DISCUSSION

Design of switch TFOs

In order to target the base adenine on either strand of a DNA duplex, we set out to study the triplex-forming properties of TFOs containing the four isomeric forms of the 2-aminopurine deoxyribonucleotides αN^{7}ap, βN^{7}ap, αN^{9}ap and βN^{9}ap, depicted in Figure 1. By molecular modeling we have identified two switch models, in which the position of the C(1′)

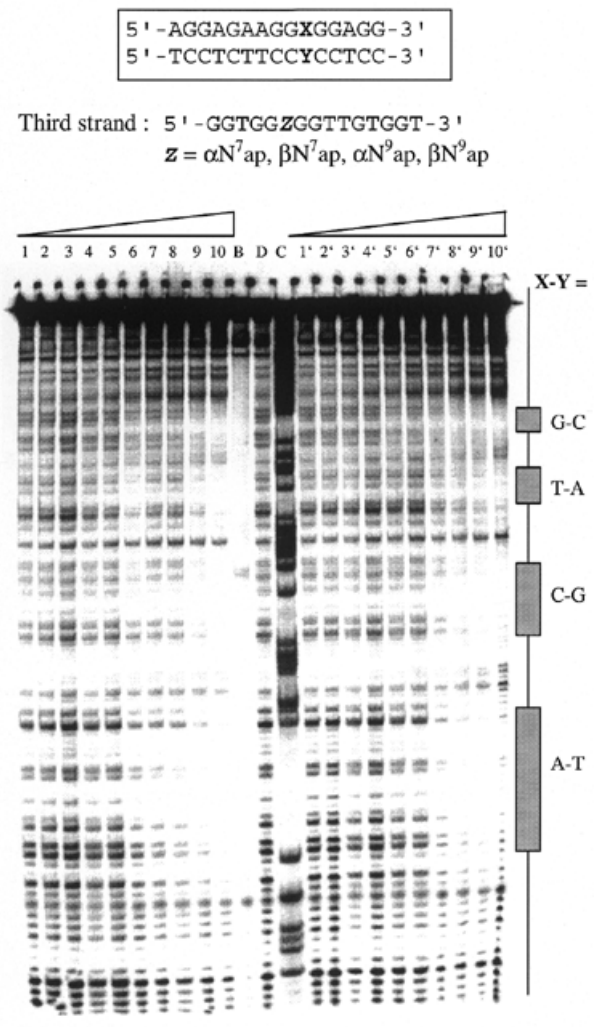

Figure 5. Top, representation of the duplex target cassettes with X-Y denoting all four natural base-pairs and TFO d(GGTGGZGGTTGTGGT), with Z representing the nucleoside units indicated. Bottom, DNase I footprinting patterns. Equilibration conditions: 10 mM bis-Tris–HCl pH 7.2, 10 mM $MgCl_2$, 1 mM spermine. Oligonucleotide concentration for lanes 1–10 (Z = αN^7ap) and 1′–10′ (Z = βN^9ap): 300 pM; 1, 3, 10, 30, 100 or 300 nM; 1, 3 or 10 μM. B, blank (no DNase I); D, only duplex; C, Maxam–Gilbert A+G-specific sequencing.

atoms between two consecutive third strand residues are located in the center of the major groove and within an acceptable distance for linkage via a phosphodiester unit. One consists of the consecutive arrangement of αN^7ap and βN^7ap nucleotides (α,β-switch) and the other of the consecutive arrangement of βN^7- and βN^9 -configured purine nucleotides (N^7,N^9-switch) (Fig. 2). Both switch models are expected to be compatible with the antiparallel (purine) triplex binding motif, in which the location of the C(1′) atoms of the third strand deoxyribose units are also located towards the center of the major groove (23).

The DNA target sequence we chose is based on the human epidermal growth hormone receptor (HER2) promoter sequence. This promoter region contains a 15 nt polypurine region which is suitable for triple helix formation. Antiparallel triplex formation with G/T-containing TFOs at this target site was investigated by Matteucci and co-workers (31). They showed by DMS footprint analysis that full protection of this site can be achieved in the absence of KCl at 1 μM concentration of TFO.

UV-melting experiments

In order to investigate triplex formation of ap-containing TFOs to the intact HER2 target sequence, we prepared the following TFOs and the DNA target duplex shown in Figure 3. In initial experiments we screened the triple helix formation potential of TFOs 1, 2, 3 and 5 (as reference) to the corresponding target duplex D1 by UV-melting curve analysis. As can be seen from Figure 4, both the βN^7ap- and αN^9ap-containing TFOs 2 and 3 bind to their target, while no triplex formation is observed in the case of the αN^7ap-containing TFO 1. Although there is no clear sigmoidal transition for melting of the third strands 2, 3 and 5 from the target duplex, we conclude that triplexes were formed in these cases from the fact that there is a clear increase in UV absorption before the melting of the double helix in duplex–TFO mixtures, and from the equal or even higher hyperchromicity relative to the duplex melting in the absence of a TFO. From these experiments it can be qualitatively inferred that both βN^7ap and αN^9ap can replace T in T × A-T base-triple formation in the antiparallel binding motif while αN^7ap cannot. This is in accord with model considerations.

DNase I footprint titration experiments

In order to assess the potential of the aminopurine-containing oligonucleotides 1–4 to recognize a T-A inversion site, and in order to evaluate their binding selectivity, a DNase I footprint titration assay (29,32) was developed. A plasmid (pSPP4C1) containing a DNA insert with the four triplex target cassettes derived from the HER2 promoter sequence (as outlined in Fig. 5, top) was prepared and used as a source of target DNA. The 247 bp *Eco*RI—*Pvu*II restriction fragment of this plasmid was 3′-end-labeled (pyrimidine-rich strand) and incubated with increasing concentrations of oligonucleotides 1–5 (300 pM to 10 μM), in 10 mM bis-Tris–HCl pH 7.2, 10 mM $MgCl_2$, 1 mM spermine at 20°C for 7 days, and then digested with DNase I. The generated reaction products were separated by denaturing gel electrophoresis and visualized by storage phosphor autoradiography. Figure 5 (bottom) shows the autoradiograms of the duplex incubated with oligonucleotide 1 (left part of the gel) and oligonucleotide 4 (right part of the gel), as an example.

The association constants (K_a) obtained for the oligonucleotides 1–5 are shown in Table 2 and the corresponding standard free energies of triplex formation ($\Delta G°$) are listed in Table 3. Possible spatial arrangements of all 16 base triples are given in Figure 6. These arrangements are based on the standard model for an antiparallel triple helix, considering *anti*-conformation around all nucleosidic bonds, and neglecting rare tautomeric or protonated forms of the aminopurine base.

By taking a closer look at the values in Table 2, it clearly appears that within the chosen sequence context, there is no strong discrimination between the different arrangements Z × X-Y. In almost all cases, binding to each target cassette could be observed. The K_a values all lie within two orders of magnitude. This seems not to be unusual for the purine motif (32) but

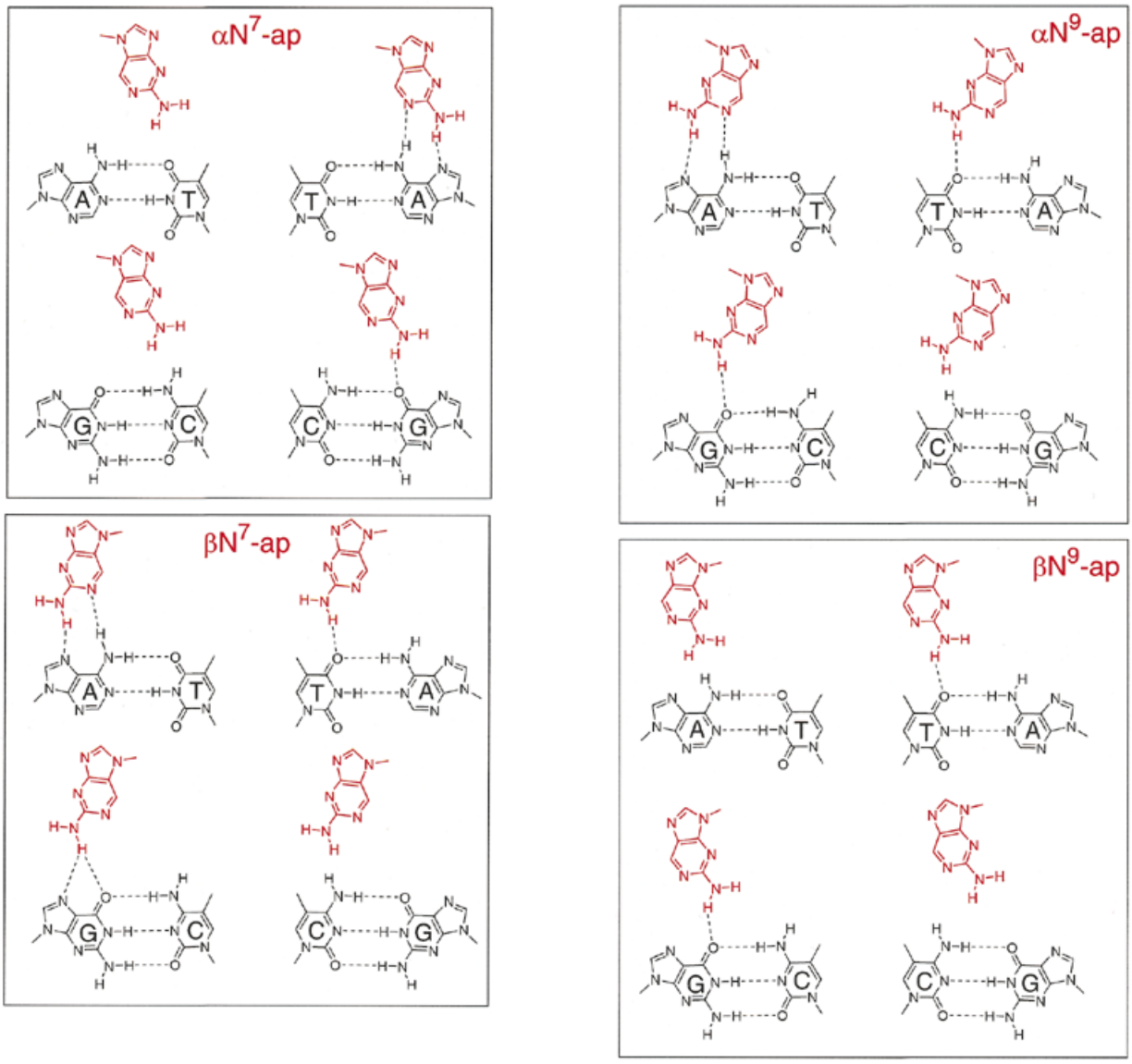

Figure 6. Spatial arrangement of all 16 base-triples investigated. For details see text.

is significantly different compared to the pyrimidine motif, where mismatched base arrangements are subject to a stronger energetic discrimination (33). As expected, the reference TFO 5 forms particularly stable triplexes with its parent adenine target. Furthermore, triple helical complexes containing the T × G-C and T × C-G have intermediate stability. This latter case was also reported by Greenberg and Dervan (32) and was attributed to specific, single hydrogen bonding contacts. In the present work under the given buffer conditions (10 mM bis-Tris–HCl pH 7.2, 10 mM $MgCl_2$, 1 mM spermine) the T × G-C base-triple is even slightly more stable than the T × C-G base-triple, which can eventually be rationalized by a bifurcated hydrogen bond between the N^7 and O^6 atoms of the guanine base.

The fact that the αN^9ap-containing TFO 3 gives the highest stability with the target sequence X-Y = A-T is probably due to the fact that this aminopurine nucleotide unit has its C(1′) atom very close to the position adopted by those of T and G within a normal, antiparallel (G/T) motif, thus giving rise to minimal distortion of the backbone. This can be inferred from molecular modeling experiments on a αN^9ap × A-T triple helix (34). Based on this reasoning, the lower affinities of the TFO 2, containing βN^7ap, for the A-T base pair, and 4, containing βN^9ap, for the T-A base pair, can also be understood. The resulting large distortions of the backbone induced by the $^{5'}$Gp(βN^7ap)$^{3'}$ and $^{5'}$(βN^7ap)p$G^{3'}$ steps seem to have a detrimental effect on stability.

A very rewarding result of the DNase I footprint experiments was the recognition of a T-A inversion site by TFO 1, containing an αN^7ap unit, as the major binding site. The K_a shows a clear, although not very pronounced, preference for the T-A over the A-T target. As in the case of the A-T recognition by TFO 3, the position of the C(1′) atom of αN^7ap is near to the position adopted by the C(1′) atom of G and T in the third strand, thus constituting nearly isomorphic base arrangements. We note, however, that the stability of TFO 1, binding to the T-A target, is less by a factor of ~4 relative to the canonical triplex

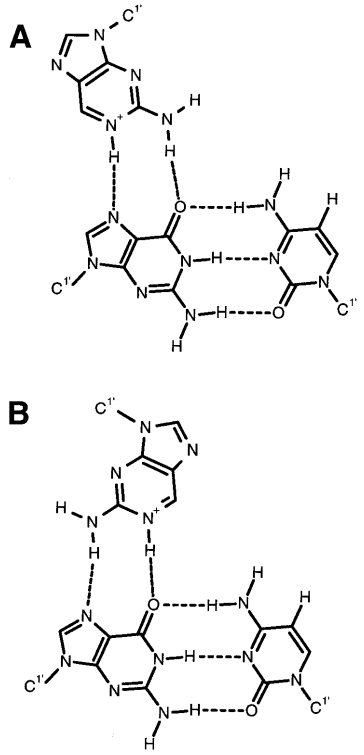

Figure 7. Hypothetical $\beta N^9apH^{+d} \times$ G-C (**A**) and $\alpha N^9apH^+ \times$ G-C (**B**) base-triples.

formed by 5 with the A-T target. Among other factors this could be due to a loss of intrastrand stacking interactions in the G-αN^7ap-G step of the TFO, and thus points towards a general problem in the switch models (Fig. 2) concerning affinity of third strands to their target (see Conclusions).

Another interesting result is the high affinity exhibited by both the αN^9- and βN^9ap-containing TFOs 3 and 4 for the G-C target. Both sequences bind with similar K_a ($1.2–1.3 \times 10^8$ M^{-1}). In contrast to the low specificity of the αN^9ap-containing TFO 3, the βN^9ap-containing TFO 4 is specific for the G-C target site with an energetic advantage of 1.0–2.8 kcal·mol^{-1} over the other three target sites. Besides the possible base arrangement given in Figure 6, the relatively high stability of the βN^9ap $\times$ G-C base triple may alternatively be rationalized by invoking protonation of the N^1 postition of the 2-aminopurine base, thus forming two hydrogen bonds with guanine (Fig. 7A). In fact, it is known from studies by Sowers *et al.* (35) on the βN^9ap-C mispair, which is at the origin of transition mutations *in vivo*, that a protonated 2-aminopurine base is engaged in this base pair (35). This could also explain the high stability of the αN^9ap $\times$ G-C base triple. In this case, the hydrogen bonds are formed between N^7(G) and H-N^2(ap) and between O^6(G) and H-N^1(ap) (Fig. 7B).

CONCLUSIONS

From the data obtained we draw the following conclusions on the utility of 2-aminopurine nucleosides for antiparallel triple-helix formation. (i) βN^7ap acts as a replacement for T (or A) in recognizing an A-T base pair. (ii) Due to the poor discrimination between the different target base-pairs X-Y, αN^9ap could eventually be further developed into a 'universal base' for antiparallel triple-helix formation. Together with the intrinsic fluorescence properties of this nucleoside (which the N^7 series is lacking) this could lead to useful diagnostic probes. (iii) The preferential recognition of a G-C base pair by βN^9ap could in principal open the way to guanine replacement in TFOs. This is of considerable interest given the fact that one of the severe limitations of the antiparallel triple-helix approach lies in the formation of G-tetrad structures of the G-rich TFOs, thus evading duplex target recognition.

The structural basis for the αN^7ap unit recognizing a T-A inversion, as set forth in the switch concept, still needs approval by high resolution structural analysis of a corresponding triplex. The question on how many inversion sites could potentially be recognized by αN^7ap-containing TFOs within a duplex target sequence also still remains open at this point. We note again that the stability of TFO 1, binding to the T-A target, is less by a factor of ~4, compared to the canonical triplex formed by 5 with the A-T target. Thus, it seems that attaining high affinity is the most important challenge in future TFO design. In this context it will be of considerable interest to combine newly discovered bases for purine–pyrimidine base-inversion recognition, as the one presented here, with overall triplex stability enhancing features, e.g. the 2-aminoethoxy sugar modification (36,37), the grafting of positive charges onto the bases (20), or both (38), in order to successfully remove the target sequence constraints in the triple-helix approach.

ACKNOWLEDGEMENT

We would like to thank the Swiss National Science Foundation for financial support of this project.

REFERENCES

1. Fox,K.R. (2000) Targeting DNA with Triplexes. *Curr. Med. Chem.*, **7**, 17–37.
2. Neidle,S. (1997) Recent developments in triple-helix regulation of gene expression. *Anticancer Drug Des.*, **12**, 433–442.
3. Moser,H.E. and Dervan,P.B. (1987) Sequence specific cleavage of double helical DNA by triple helix formation. *Science*, **238**, 645–650.
4. François,J.-C., Saison-Behmoaras,T. and Hélène,C. (1988) Sequence-specific recognition of the major groove of DNA by oligodeoxynucleotides via triple helix formation. Footprinting studies. *Nucleic Acids Res.*, **16**, 11431–11440.
5. Beal,P.A. and Dervan,P.B. (1991) Second structural motif for recognition of DNA by oligonucleotide directed triple-helix formation. *Science*, **251**, 1360–1363.
6. Durland,R.H., Kessler,D.J., Gunnell,S., Duvic,M., Pettitt,B.M. and Hogan,M.E. (1991) Binding of triple helix forming oligonucleotides to sites in gene promoters. *Biochemistry*, **30**, 9246–9255.
7. Gowers,D.M. and Fox,K.R. (1999) Towards mixed sequence recognition by triple helix formation. *Nucleic Acids Res.*, **27**, 1569–1577.
8. Sun,J.S., De Bizemont,T., Duval-Valentin,G., Montenay-Garestier,T. and Hélène,C. (1991) Extension of the range of recognition sequences for triple helix formation by oligonucleotides containing guanines and thymines. *C.R. Acad. Sci. III*, **313**, 585–590.
9. Beal,P.A. and Dervan,P.B. (1992) Recognition of double helical DNA by alternate strand triple helix formation. *J. Am. Chem. Soc.*, **114**, 4976–4982.
10. Horne,D.A. and Dervan,P.B. (1990) Recognition of mixed-sequence duplex DNA by alternate-strand triple-helix formation. *J. Am. Chem. Soc.*, **112**, 2435–2437.
11. Ono,A., Chen,C.-N. and Kan,L.-S. (1991) DNA triplex formation of oligonucleotide analogues consisting of linker groups and octamer

segments that have opposite sugar-phosphate backbone polarities. *Biochemistry*, **30**, 9914–9921.
12. De Bizemont,T., Duval-Valentin,G., Sun,J.-S., Bisagni,E., Garestier,T. and Hélène,C. (1996) Alternate strand recognition of double-helical DNA by (T,G)-containing oligonucleotides in the presence of a triple helix-specific ligand. *Nucleic Acids Res.*, **24**, 1136–1143.
13. Zhou,B.-W., Marchand,C., Asseline,U., Thuong,N.T., Sun,J.-S., Garestier,T. and Hélène,C. (1995) Recognition of alternating oligopurine/oligopyrimidine tracts of DNA by oligonucleotides with base-to-base linkages. *Bioconjugate Chem.*, **6**, 516–523.
14. Asseline,U. and Thuong,N.T. (1994) 5′-5′ tethered oligonucleotides via nucleic bases: a potential new set of compounds for alternate strand triple-helix formation. *Tetrahedron Lett.*, **35**, 5221–5224.
15. Asseline,U. and Thuong,N.T. (1993) Oligonucleotides tethered via nucleic bases. A potential new set of compounds for alternate strand triple-helix formation. *Tetrahedron Lett.*, **34**, 4173–4176.
16. Lehmann,T.E., Greenberg,W.A., Liberles,D.A., Wada,C.K. and Dervan,P.B. (1997) Triple-helix formation by pyrimidine oligonucleotides containing nonnatural nucleosides with extended aromatic nucleobases: Intercalation from the major groove as a method for recognizing C.G and T.A base-pairs. *Helv. Chim. Acta*, **80**, 2002–2022.
17. Huang,C.-Y., Cushman,C.D. and Miller,P.S. (1993) Triplex formation by an oligonucleotide containing N4-(3-amidopropyl)cytosine. *J. Org. Chem.*, **58**, 5048–5049.
18. Stilz,H.-U. and Dervan,P.B. (1993) Specific recognition of CG base pairs by 2-deoxynebularine within the purine·purine·pyrimidine triple-helix motif. *Biochemistry*, **32**, 2177–2185.
19. Amosova,O. and Fresco,J.R. (1999) A search for base analogs to enhance third-strand binding to 'inverted' target base-pairs of triplexes in the pyrimidine/parallel motif. *Nucleic Acids Res.*, **27**, 4632–4635.
20. Gowers,D.M., Bijapur,J., Brown,T. and Fox,K.R. (2000) DNA triple helix formation at target sites containing several pyrimidine interrupts: stabilization by protonated cytosine or 5-(1-propargylamino)dU. *Biochemistry*, **38**, 13747–13758.
21. Prévot-Halter,I. and Leumann,C. (1999) Selective recognition of a C-G base-pair in the parallel DNA triple-helical binding motif. *Bioorg. Med. Chem. Lett.*, **9**, 2657–2660.
22. Marfurt,J. and Leumann,C. (1998) Evidence for CH···O hydrogen bond assisted recognition of a pyrimidine base in the parallel DNA triple helical motif. *Angew. Chem. Inl. Ed Engl.*, **37**, 175–177.
23. Thuong,N.T. and Hélène,C. (1993) Sequence specific recognition and modification of double helical DNA by oligonucleotides. *Angew. Chem. Intl. Ed. Engl.*, **32**, 666–690.
24. Doronina,S.O., Blanalt-Feidt,S. and Behr,J.-P. (1999) DNA recognition by non-natural oligonucleotides. *Nucl. Nucl.*, **18**, 1617–1618.
25. Doronina,S.O. and Behr,J.-P. (1998) Synthesis of 4-guanidinopyrimidine nucleosides for triple helix-mediated guanine and cytosine recognition. *Tetrahedron Lett.*, **39**, 547–550.
26. Parel,S.P. and Leumann,C.J. (2000) Synthesis and pairing properties of oligodeoxynucleotides containing N7-(purine-2-amine deoxynucleosides). *Helv. Chim. Acta*, **83**, 2514–2526.
27. Wu,X. and Pitsch,S. (1998) Synthesis and pairing properties of oligoribonucleotide analogues containing a metal-binding site attached to β-D-allofuranosyl cytosine. *Nucleic Acids Res.*, **26**, 4315–4323.
28. Sambrook,J., Fritsch,E.F. and Maniatis,T. (1989) *Molecular Cloning: A Laboratory Manual*. Cold Spring Harbor Laboratory Press. Cold Spring Harbor, NY.
29. Brenowitz,M., Senear,D.F., Shea,M.A. and Ackers,G.K. (1986) Quantitative DNase footprint titration: a method for studying protein–DNA interactions. *Methods Enzymol.*, **130**, 132–181.
30. Priestley,E.S. and Dervan,P.B. (1995) Sequence composition effects on the energetics of triple helix formation by oligonucleotides containing a designed mimic of protonated cytosine. *J. Am. Chem. Soc.*, **117**, 4761–4765.
31. Milligan,J.F., Krawczyk,S.H., Wadwani,S. and Matteucci,M.D. (1993) An antiparallel triple helix motif with oligodeoxynucleotides containing 2′-deoxyguanosine and 7-deaza-2′-deoxyxanthosine. *Nucleic Acids Res.*, **21**, 327–333.
32. Greenberg,W.A. and Dervan,P.B. (1995) Energetics of sixteen triple helical complexes which vary at a single position within a purine motif. *J. Am. Chem. Soc.*, **117**, 5016–5022.
33. Best,G.C. and Dervan,P.B. (1995) Energetics of formation of sixteen triple helical complexes which vary at a single position within a pyrimidine motif. *J. Am. Chem. Soc.*, **117**, 1187–1193.
34. Parel,S.P. (2000) 2-Aminopurine nucleotides in DNA-triplex formation: selective recognition of a T-A base-pair in the antiparallel recognition motif. PhD Thesis, University of Berne, Switzerland.
35. Sowers,L.C., Boulard,Y. and Fazakerley,G.V. (2000) Multiple structures for the 2-aminopurine–cytosine mispair. *Biochemistry*, **39**, 7613–7620.
36. Blommers,M.J.J., Natt,F., Jahnke,W. and Cuenoud,B. (1998) Dual recognition of double-stranded DNA by 2′-aminoethoxy-modified oligonucleotides: the solution structure of an intramolecular triplex obtained by NMR spectroscopy. *Biochemistry*, **37**, 17714–17725.
37. Cuenoud,B., Casset,F., Hüsken,D., Natt,F., Wolf,R.M., Altmann,K.-H., Martin,P. and Moser,H.E. (1998) Dual recognition of double-stranded DNA by 2′-aminoethoxy-modified oligonucleotides. *Angew. Chem. Intl. Ed. Engl.*, **37**, 1288–1291.
38. Sollogoub,M., Dominguez,B., Fox,K.R. and Brown,T. (2000) Synthesis of a novel bis-amino-modified thymidine monomer for use in DNA triplex stabilisation. *Chem. Commun.*, 2315–2316.